Environmental Health Perspectives
Vol. 68, pp. 81-89, 1986

Pathology of Aging Female SENCAR Mice Used as Controls in Skin Two-Stage Carcinogenesis Studies

by Jerrold M. Ward,* Ricardo Quander,*† Deborah Devor,‡ Martin L. Wenk,‡ and Edwin F. Spangler‡

The pathology of 60 aged female SENCAR mice used as acetone controls in skin painting studies was studied. Fifty percent of the mice survived past 96 weeks of age. The major contributing causes of death identified in 42 mice were glomerulonephritis (8 mice), histiocytic sarcoma (7 mice), and other tumors (8 mice). Glomerulonephritis was found in the majority of mice and was associated with thymic hyperplasia, focal vasculitis, and lymphoid hyperplasia. Necropsy of 58 mice surviving past 50 weeks of age revealed that 41 had an average of 1.36 tumors per mouse. The most common tumors included histiocytic sarcoma (13 mice), pulmonary adenoma or adenocarcinoma (11 mice), mammary tumors (11 mice), follicular center cell lymphoma (4 mice), and hepatocellular adenoma (4 mice). The 13 histiocytic sarcomas appeared to arise in the uterus and metastasized to liver (9 mice), lung (4 mice), kidney (3 mice), and other tissues. Lung tumors were of the solid and papillary types, and tumor cells frequently contained surfactant apoprotein (SAP) but did not contain Clara cell antigens, suggesting their origin from alveolar Type II cells. A variety of nonneoplastic lesions, similar to those observed in other mouse strains, were seen in other tissues of these mice. Amyloid-like material was seen only in nasal turbinates and thyroid gland.

In a group of 28 mice exposed to 12-O-tetradecanoylphorbol-13-acetate (TPA) for up to 88 weeks, as a control for other treatment groups, 7 (25%) had papillomas and 5 (17.8%) had squamous cell carcinomas of the skin at necropsy, although many other induced papillomas regressed during the study.

Introduction

SENCAR mice were bred for increased sensitivity to skin initiation and promotion protocols (*1–3*). They originated in 1959 from Rockland all-purpose mice that were inbred for sensitivity to skin initiation by 7,12-dimethylbenz[a]anthracene (DMBA) and promotion by croton oil. In 1971, these susceptible mice were outbred with Charles River CD-1 mice to produce hybrid vigor. These mice have been bred at Oak Ridge National Laboratory for use in skin carcinogenesis studies of 6 to 12 months duration. There have been no reports on the pathology of aging SENCAR mice, although several studies of the CD-1 mouse have been published (*4,5*). As part of a large study to characterize the possible skin initiating and promoting activities of formaldehyde (*6*), we maintained groups of female SENCAR mice for up to 100 weeks of age. There was no evidence that any of the tumors or lesions in these mice were associated with their exposure to acetone; they were considered to occur naturally. In this paper, we describe the pathology of these aged mice.

Materials and Methods

For a large study to test the skin initiating or promoting properties of formaldehyde, 260 female SENCAR mice were obtained from Oak Ridge National Laboratory Animal Resources (Oak Ridge, TN) at 7 weeks of age. Sixty of these mice were used for the present study. They were placed in polycarbonate cages, 11.5 × 7.5 × 5 in. in size, on corn cob bedding. Water and Purina Lab Chow were available *ad libitum*. For 30 mice in experimental group 4B, 0.2 mL of a 10% formalin solution (37–40% formaldehyde solution in acetone) was applied once to the back at 8 weeks of age. Four weeks later, 0.2 mL acetone was applied once weekly for 88 weeks. For 30 mice in experimental group 4D, 0.2 mL of acetone was applied twice weekly to their backs from 8 weeks of age for 92 weeks. These mice were weighed monthly. No untreated mice were available for aging studies. These groups are combined because all neoplastic and nonneoplastic lesions occurred with similar incidence in both groups and surival was similar. All surviving mice were sacrificed at 101 to 102 weeks of age, 93 to 94 weeks after initiation of the study.

*Tumor Pathology and Pathogenesis Section, Laboratory of Comparative Carcinogenesis, Division of Cancer Etiology, National Cancer Institute, Frederick, MD 21701.
†Present address: Hazelton Laboratories, Vienna, VA 22180.
‡Microbiological Associates, Bethesda, MD 20816.

After arrival from the supplier and at terminal sacrifice (100 weeks of age), serum samples were obtained from 2 and 15 mice, respectively, and sent to the Comprehensive Health Service of Microbiological Associates (Bethesda, MD). These samples were surveyed by hemaglutination-inhibition (HI) to test for antibodies to the following viruses: PVM, Sendai, Reo 3, K, polyoma, MVM, and GDVII; by complement fixation to test for antibodies to mouse adenovirus and LCM; and by ELISA to test for antibodies to MVM, PVM, Sendai, Ectromelia, and GDVII.

A complete necropsy examination was performed on each mouse. The majority of the major organs and gross lesions were fixed in 10% neutral buffered formalin. All major tissues, gross lesions, and selected other tissues were embedded in paraffin, and sections were cut at 4 to 6 μm and stained with hematoxylin and eosin. For selected tissues, the avidin biotin peroxidase-complex (ABC) immunocytochemical technique was used (*7,8*) with the Vectastain kits (Vector Laboratories, Burlingame, CA) to localize specific antigens with the use of antibodies to surfactant apoprotein (SAP) (*7*), Clara cell antigen (*7*), prolactin (National Hormone and Pituitary Program, Baltimore, MD), insulin (Miles Laboratories, Elkhart, IN), glucagon (DAKO Corp., Santa Barbara, CA), S-100 (DAKO Corp.), somatostatin (DAKO Corp.), lysozyme (DAKO Corp.), α_1-antitrypsin (DAKO Corp.), biotinylated antimouse IgG (Vector Laboratories), mouse lambda and kappa immunoglobulin light chains (Litton Bionetics, Charleston, SC), or vimentin (Transformation Research, Inc., Framingham, MA). For localization of immunoglobulins or immunoglobulin light chains, tissue sections were trypsinized first.

Portions of selected formalin-fixed kidneys were placed in glutaraldehyde, embedded in epoxy resin, sectioned, stained with uranyl acetate and lead citrate, and viewed under an electron microscope.

Results

Body Weights, Serology, and Survival

The mean body weight curve of mice in groups 4B and 4D is shown in Figure 1. The mean weight of mice steadily rose throughout their lifespan, reaching 49 g at 100 weeks of age. Although two mice died or were sacrificed before 16 weeks of age, the next one died at 52 weeks of age and 50% survived to 96 weeks of age (Fig. 2). Forty-four mice died or were sacrificed in moribund condition during the study.

Serology performed on the two mice at the time of arrival from the supplier showed that their sera did not demonstrate murine viral antibodies. At the end of the study, sera from 15 aged mice, when tested using ELISA, contained significant serum viral antibody titers to MHV (14/15), Sendai virus (6/6), MVM (6/6); and when tested using HI, to PVM (2/15), Sendai virus (12/15), and MVM (10/15). Other serological tests were negative.

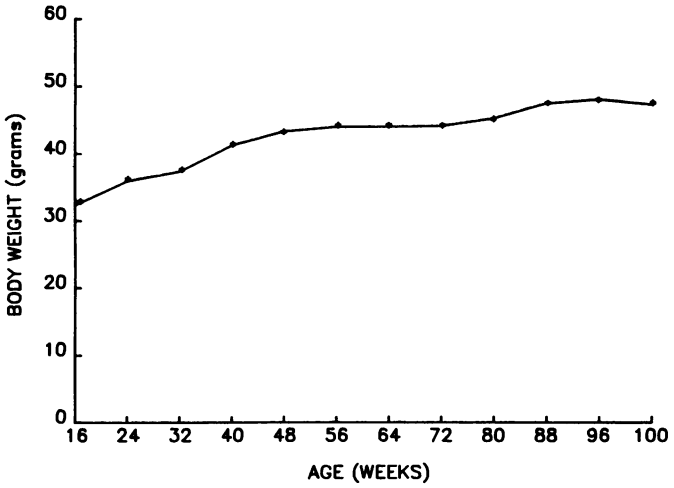

FIGURE 1. Mean body weight gain of 60 female SENCAR mice used as acetone controls in a skin initiation-promotion experiment.

Pathology

Contributing Causes of Death. The major contributing causes of illness or death in 42 mice are presented in Table 1. These determinations were based on gross and microscopic findings. Of these mice, 35% died from the effects of tumors, and 64% died from other causes. Glomerulonephritis was a major cause of death in eight mice, and two of these mice had generalized edema (nephrotic syndrome). Histiocytic sarcoma arising in the uterus and spreading to other tissues was the major lethal tumor type.

Neoplastic and Nonneoplastic Lesions. Of the 58 mice surviving past 52 weeks of age, 41 (70.6%) had an average of 1.36 tumors per mouse (Table 2). Many mice had a variety of nonneoplastic lesions as shown in Table

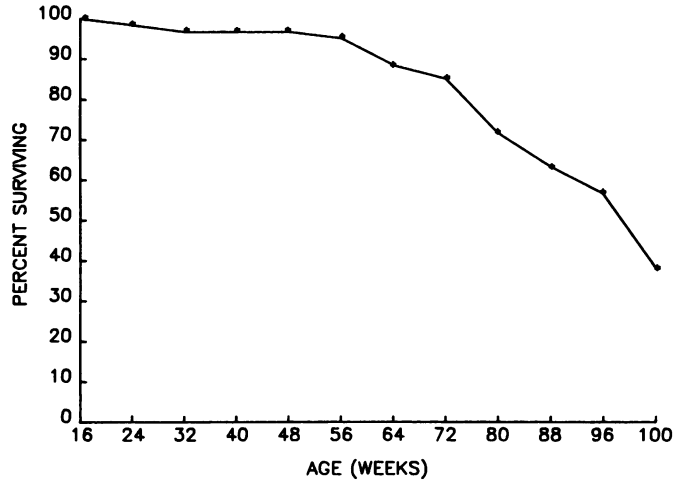

FIGURE 2. Survival of 58 female SENCAR mice living past 16 weeks of age. Fifty percent survived to 96 weeks of age.

Table 1. Contributing causes of death of 42 aging female SENCAR mice.

Lesion	No. affected (%)
Neoplastic	15 (35.7)
Histiocytic sarcoma	7 (16.6)
Lymphoma	3 (7.1)
Pulmonary adenocarcinoma	2 (4.7)
Mammary adenocarcinoma	2 (4.7)
Pituitary adenoma	1 (2.3)
Nonneoplastic	27 (64.3)
Glomerulonephritis	8 (19.0)
Hemoperitoneum	3 (7.1)
Necrotizing enteritis	2 (4.7)
Peritonitis	1 (2.3)
Necrotizing metritis	1 (2.3)
Hemothorax	1 (2.3)
Cachexia	1 (2.3)
Septicemia	1 (2.3)
Undetermined	9 (21.4)

3. The major lesions and some unusual lesions are described according to organ system. One mouse receiving acetone twice weekly for 88 weeks had a papilloma at the site of application that appeared only at 92 weeks.

Kidney. The primary renal lesion consisted of glomerulonephritis with a variety of secondary lesions. Glomerular lesions were scored as mild, moderate, or severe, depending on their extent and severity. In general, within a given kidney, glomeruli exhibited a variety of changes consisting of increased mesangial matrix and mesangial cells, thickened capillary loops, sclerosis, and hypertrophy of mesangial cell nuclei (Fig. 3). Some glomeruli were involved in more acute processes characterized by fibrin deposition, mild neutrophilic infiltrate, and individual cell necrosis. A few cases had crescent formation, fibrosis, and obliteration of glomerular tufts. Immunocytochemically, we demonstrated mouse IgG and immunoglobulin kappa light chains within thickened glomerular capillary loops and within the mesangium (Fig. 4) after trypsinization of formalin-fixed kidney sections. Ultrastructurally, subendothelial and subepithelial electron-dense deposits were seen within thickened glomerular basement membranes (Fig. 5). Obliteration of epithelial foot processes was also observed. Severe tubular degeneration and hyaline cast formation, although present in several animals, was not a prominent feature in most mice. The majority of mice, however, did have mild to marked lymphocytic and plasma cell perivascular cuffs around intrarenal arteries.

Hematopoietic System. Follicular center cell (B-cell) lymphomas of spleen and lymph nodes were found in four mice. With trypsinization of formalin-fixed tissue sections, immunoglobulin was seen focally within tumor cells. The primary nonneoplastic lesions involving the lymphoreticular system consisted of mild to severe lymphoid cell hyperplasia of both B- and T-cell zones. The thymuses in nearly all mice were very prominent (excessively so for 1- to 2-year-old mice) and had a mixture of cortical and medullary (follicular) lymphoid cell hyperplasia together with the proliferation of medullary epithelial cells and sometimes with small cyst formation. The spleens exhibited varying degrees of periarterial lymphoid sheath hyperplasia with associated lymphoid follicles. Also, the amount of myeloid metaplasia in the red pulp was frequently excessive. Lymph nodes sim-

Table 2. Neoplastic lesions in 58 aging female SENCAR mice.

Tissue Tumor	No. affected (%)
Hematopoietic	
Lymphoma (follicular center cell)	4 (6.8)
Spleen	4
Lymph nodes	4
Thymus	3
Lymphoma (other)	1 (1.7)
Reproductive tract	
Histiocytic sarcoma	13 (22.4)
Uterus	13
Liver	9
Lung	4
Kidney	3
Lymph node	2
Ovary	2
Pancreas	1
Small intestine	1
Adrenal	1
Uterus	
Leiomyosarcoma	2 (3.4)
Endometrial polyp	2 (3.4)
Fibroma	1 (1.7)
Adenocarcinoma	1 (1.7)
Lung	
Primary tumors	11 (18.9)
Adenoma, solid	6
Adenoma, papillary	3
Adenocarcinoma, papillary	2
Metastatic tumors	
Mammary adenocarcinoma	2 (3.4)
Endocrine	
Pituitary gland	
Adenoma	3 (5.1)
Thyroid gland	
Follicular adenoma	2 (3.4)
Adrenal gland	
Cortical carcinoma	1 (1.7)
Pheochromocytoma	1 (1.7)
GI tract	
Tongue	
Papilloma	1 (1.7)
Stomach	
Polypoid adenoma	2 (3.4)
Small intestine	
Adenoma	1 (1.7)
Liver	
Hepatocellular adenoma	4 (6.8)
Hemangiosarcoma	1 (1.7)
Hemangioma	1 (1.7)
Skin	
Papilloma	1 (1.7)
Mammary gland	
Adenocarcinoma	11 (18.9)
Type A	4
Type B	5
Adenoacanthoma	1
Fibrosarcoma	2
In situ ductal carcinoma	1
Harderian gland	
Adenoma	3 (5.1)

Table 3. Nonneoplastic lesions of 58 aging female SENCAR mice.

Tissue	Lesion	No. affected/no. tissues examined histologically (%)
Kidney	Glomerulonephritis	48/58 (82.7)
	Mild	14/58 (24.1)
	Moderate	20/58 (34.4)
	Severe	14/58 (24.1)
	Perivascular chronic inflammation	39/58 (67.2)
Hematopoietic		
Thymus	Lymphoid and epithelial hyperplasia	34/38 (89.4)
	Medullary cyst	12/38 (31.5)
Spleen	Myeloid metaplasia	46/57 (80.7)
	Lymphoid hyperplasia	36/57 (63.1)
	Hemosiderosis	5/57 (8.7)
Lymph nodes	Lymphoid hyperplasia	23/38 (60.5)
	Plasmacytosis	9/42 (21.4)
	Myeloid metaplasia	5/42 (11.9)
	Sinus histiocytosis	2/42 (4.7)
Liver	Cytomegaly	36/56 (64.2)
	Coagulative necrosis, focal	11/56 (19.6)
	Chronic cholangitis	34/56 (60.7)
	Acute cholangitis	8/56 (14.2)
	Granulomas	9/56 (19.6)
	Mitotic figures	5/56 (8.9)
	Fatty change	2/56
	Biliary cyst	3/56 (5.3)
	Basophilic hepatocellular focus	2/56 (3.5)
Respiratory tract		
	Nasal turbinates	
	Amyloidosis	18/23 (78.2)
	Chronic inflammation	3/23 (13.0)
	Lung	
	Perivascular lymphoid hyperplasia	19/56 (33.9)
	Peribronchiolar lymphoid hyperplasia	15/56 (26.7)
	Interstitial pneumonia	7/56 (12.5)
	Bronchiolitis	1/56 (1.7)
Reproductive tract		
Uterus		
	Cystic endometrial hyperplasia	44/53 (83.0)
	Necrotizing metritis	1/53 (1.8)
Ovary		
	Simple cyst	20/22 (90.9)
	Hematoma	1/22 (4.5)
Endocrine		
Adrenal gland		
	Subcapsular spindle cell hyperplasia	34/44 (77.2)
	Focal cortical hyperplasia	4/44 (9.0)
Thyroid gland		
	Amyloidoisis	3/38 (7.8)
Pancreas		
	Islet cell hyperplasia	17/48 (35.4)
	Inflammation	8/48 (16.6)
	Acinar cell vacuolation	2/48 (4.1)
	Atrophy	1/48 (2.0)
	Inflammation, islets	1/48 (2.0)
Lacrimal gland	Dacryoadenitis	9/13 (69.2)
Blood vessels		
	Vasculitis	18/56 (32.1)
	Arteritis, aorta	10/56 (17.8)
	Aorta, rupture	1/56 (1.7)
Heart	Fibrosis, focal	5/56 (8.9)

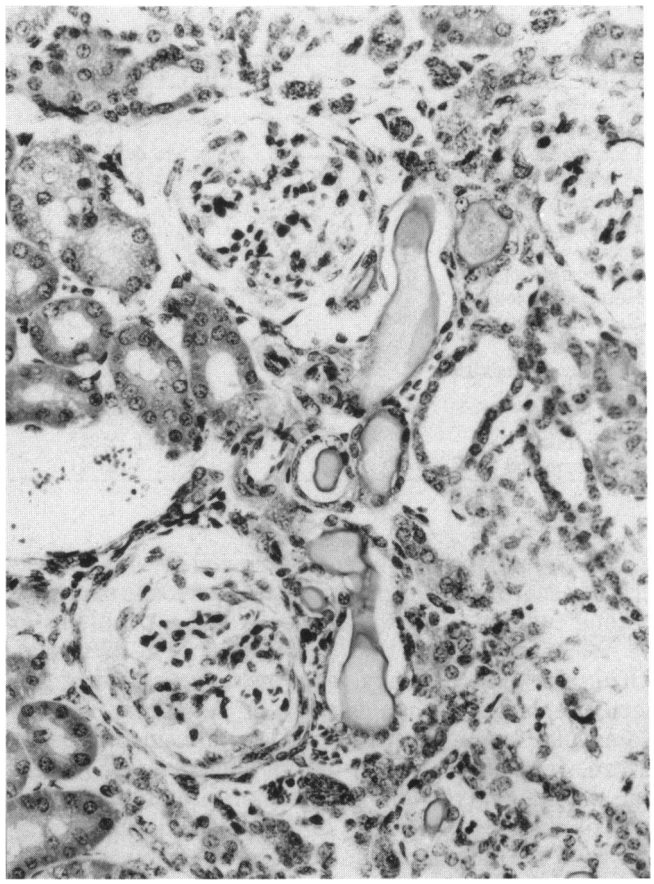

FIGURE 3. Glomerulonephritis in a female SENCAR mouse. Hematoxylin and eosin (H & E), ×250.

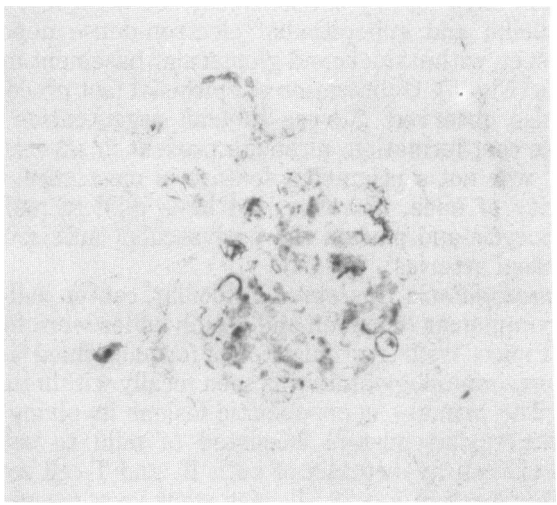

FIGURE 4. Kappa immunoglobulin light chains concentrated in glomerular capillary loops and mesangium. ABC immunoperoxidase, trypsinization, H & E, ×400.

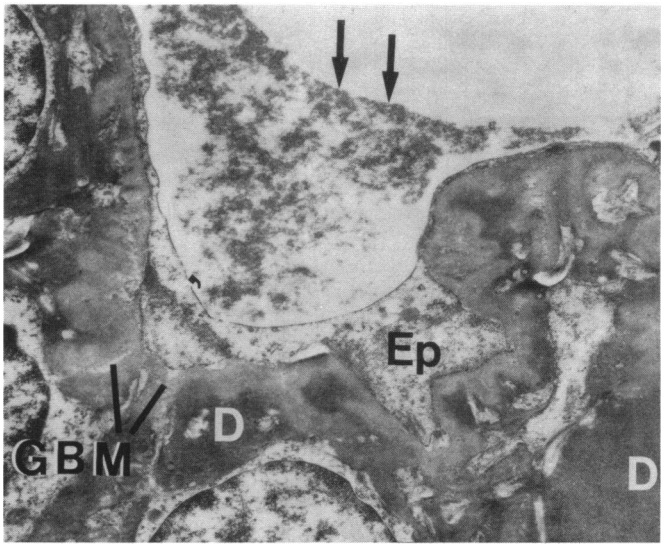

FIGURE 5. Ultrastructural demonstration of thickened glomerular basement membranes (GBM) electron dense deposits (D) and obliteration of epithelial (EP) foot process. Uranyl acetate and lead citrate, ×7400.

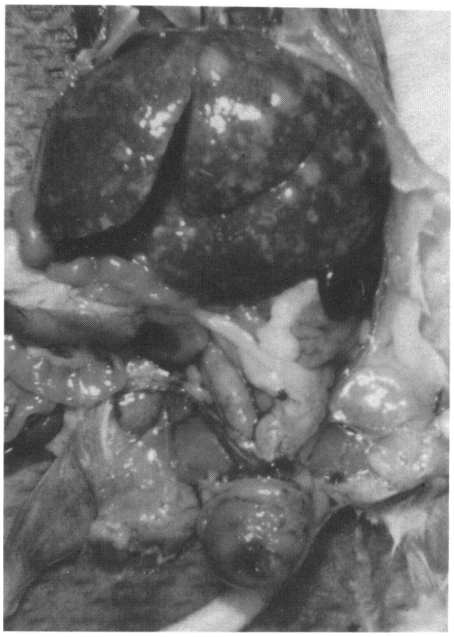

FIGURE 7. Histiocytic sarcoma arising within vagina and cervix and metastasizing to the liver.

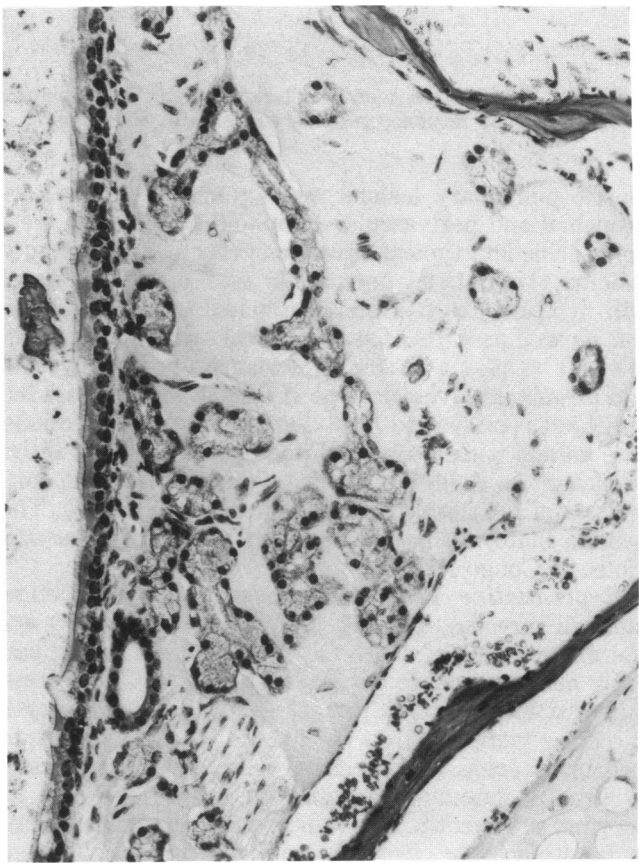

FIGURE 6. Amyloidosis in subepithelial layer of respiratory nasal region. H & E, ×250.

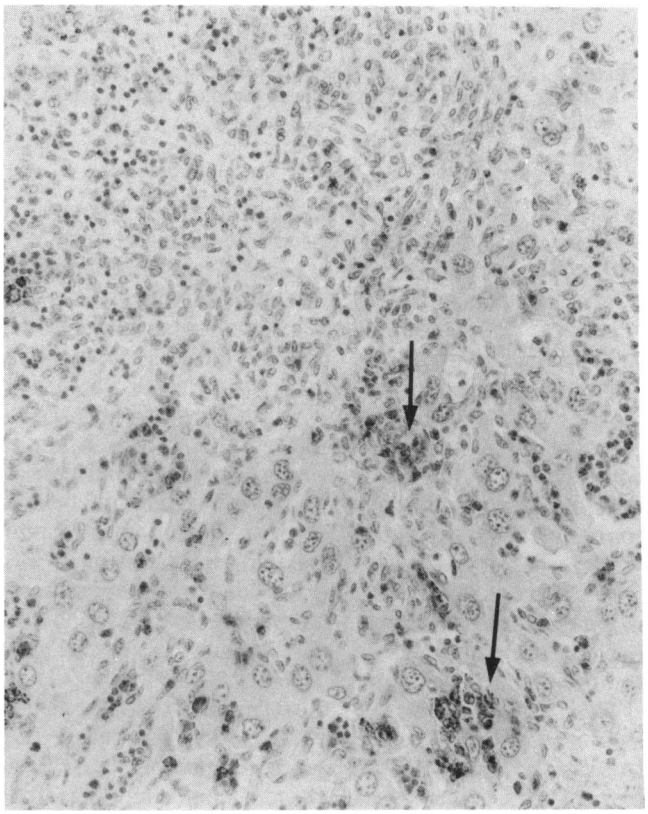

FIGURE 8. Histiocytic sarcoma in liver of SENCAR mouse. α_1-Antitrypsin was found in only a few tumor cells (arrows). ABC immunoperoxidase and hematoxylin, ×250.

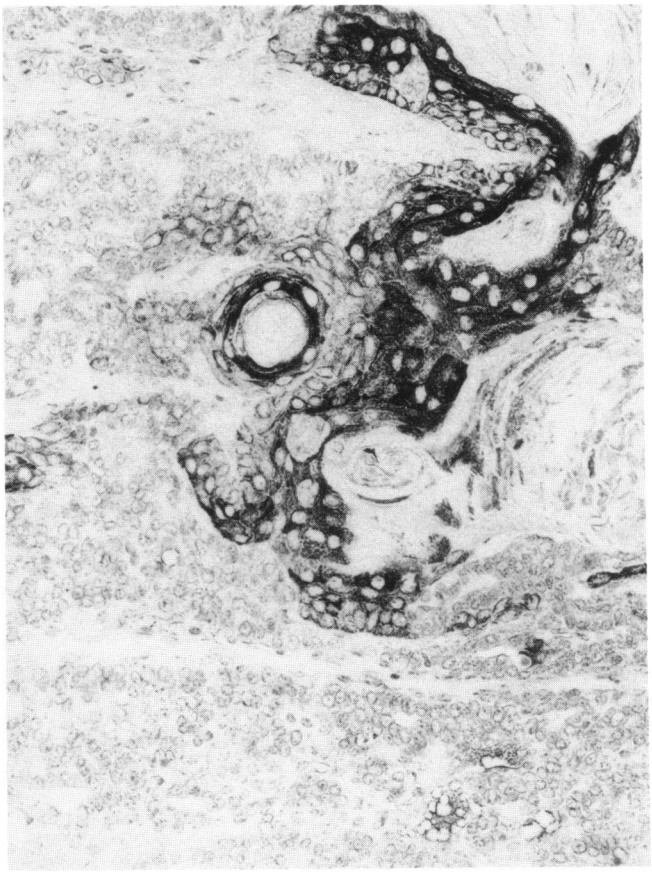

FIGURE 9. Keratin in areas of squamous metaplasia of a mammary adenoacanthoma. ABC immunoperoxidase and hematoxylin, ×250.

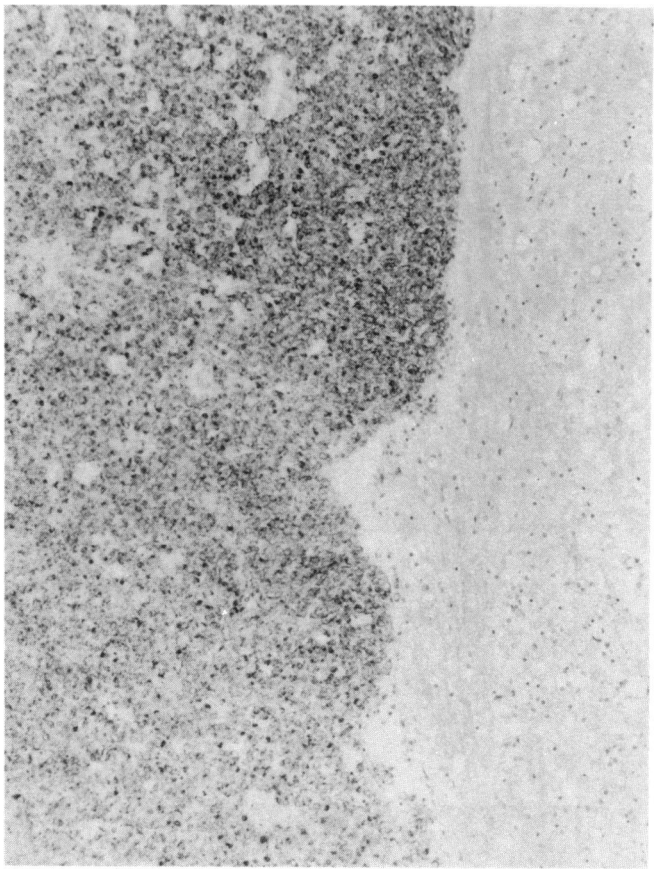

FIGURE 10. Prolactin in a pituitary tumor invading into brain parenchyma. ABC immunoperoxidase and hematoxylin, ×100.

ilarly exhibited follicular and paracortical hyperplasia together with varying degrees of plasmacytosis. Myeloid metaplasia was also present in several nodes as well. These mice did not have skin tumors.

Liver. Four hepatocellular adenomas and two basophilic foci were found in these mice. Generally, all nonneoplastic lesions noted were very mild. Patterns of focal necrosis varied from individual cell to larger, discrete portions of hepatic lobules, suggestive of ischemia. Livers with individual cell necrosis often had concurrent, mild, dense focal infiltrates of neutrophils or macrophages forming small, discrete granulomas. Livers with ischemic necrosis often had marked tumor infiltrate. Chronic inflammatory lesions consisted primarily of small, densely cellular focal infiltrates of lymphocytes with lesser numbers of plasma cells in portal areas around central veins or in parenchyma.

Respiratory Tract. Lung tumors displayed both solid and papillary patterns (Table 2). The tumor cells frequently contained surfactant apoprotein (SAP), but never Clara cell antigen, when stained using the ABC technique. Of two solid tumors stained, both were immunoreactive for SAP and of five papillary tumors, one had foci of intranuclear reactivity for SAP. Nonneoplastic pulmonary lesions were generally mild. Peribronchial and perivascular lymphoid hyperplasia were nonspecific and typical of lesions present in many aged rodents. Interstitial pneumonia was often associated with lymphoid cuffs around bronchioles and blood vessels as well as with small multifocal areas of thickened alveolar septae with mononuclear inflammatory cells and prominent alveolar Type II cells. Some of these foci may have represented resolving Sendai virus infections. One animal with interstitial pneumonia also had active bronchiolitis. A high incidence (78%) of apparent amyloidosis of the nasal turbinates was seen (Fig. 6). This hyaline material, however, did not stain with crystal violet or Congo red.

Reproductive Tract. Histiocytic sarcoma (reticulum cell sarcoma, Type A; lymphoma, histiocytic) was the major cause of death (seven mice) and had apparently metastasized to several organs (Fig. 7). Thirteen mice (22.4%) had this tumor. A few early histiocytic sarcomas were found in the uterus. We found α_1-antitrypsin in some tumor cells (Fig. 8) of a few tumors, using ABC immunocytochemistry, but never S-100, lysozyme, or vimentin. One tumor was easily transplanted and cultivated *in vitro*. The rounded tumor cells grew very slowly *in vitro* but grew quickly into tumors when transplanted *in vivo*.

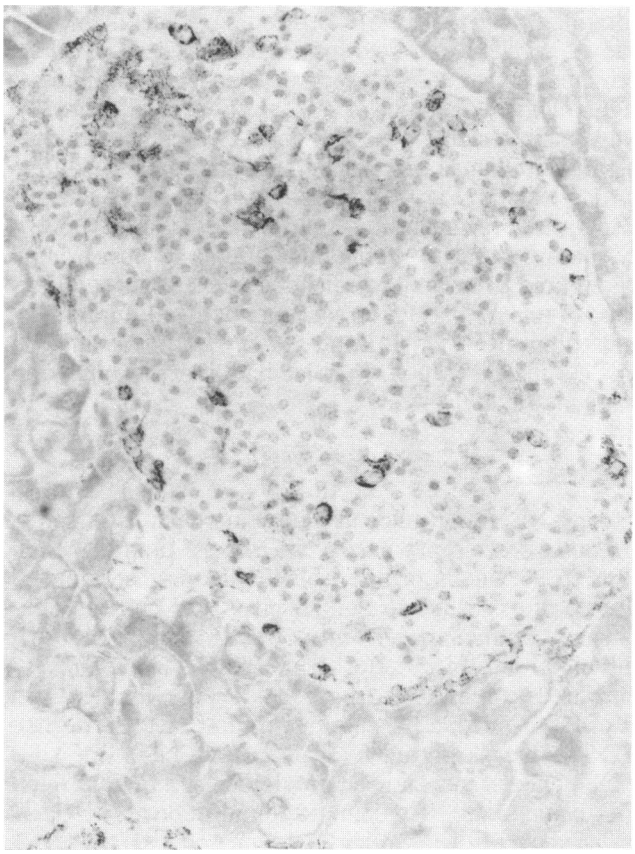

FIGURE 11. Glucagon in a hyperplastic pancreatic islet. The majority of the islet cells contained immunoreactive insulin, ABC immunoperoxidase and hematoxylin, ×250.

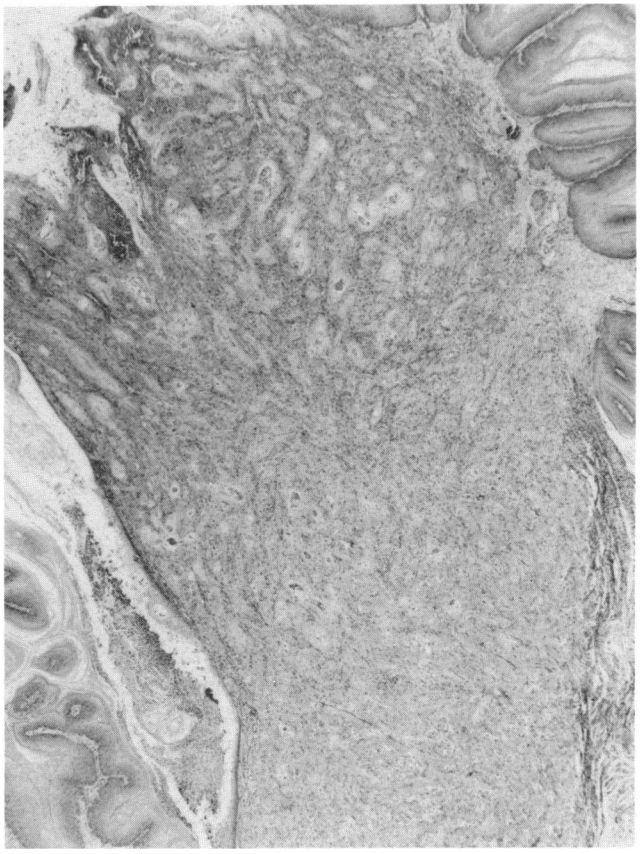

FIGURE 13. Poorly differentiated squamous cell carcinoma arising within a papilloma of a SENCAR mouse receiving TPA. H & E, ×40.

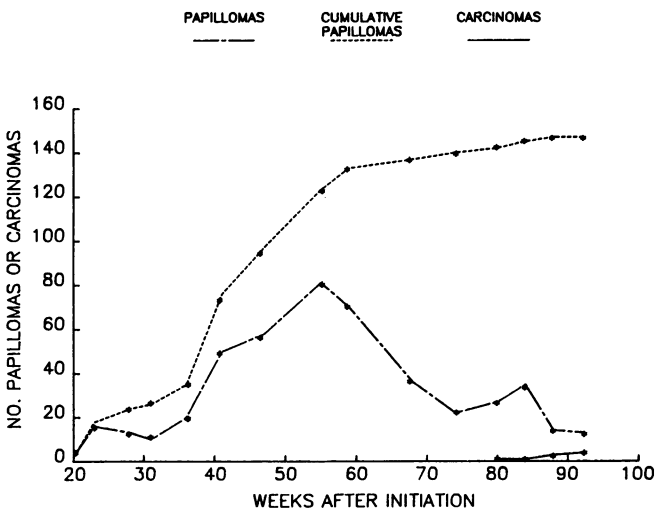

FIGURE 12. Skin papillomas and carcinomas seen clinically in female SENCAR mice receiving TPA, 1.25 μg once weekly, for 88 weeks. The decrease in papillomas was primarily due to regression of the lesions and also to mortality.

Uterine cystic endometrial hyperplasia was typical of that found in aged female rodents and varied from mild to severe with complete distortion of uterine architecture. One mouse had a severe necrotizing metritis, which contributed to early death. Ovarian cysts were present in nearly all animals and ranged from small cysts to very large thin-walled structures with complete loss of normal ovarian tissue. In many animals, a large cystic mass, distended with clotted blood, was present, often reaching up to 1 cm in diameter. Focal angiectasis was observed on the edge of a few of these hemorrhagic lesions.

Thirteen mammary tumors were found in eleven mice. After trypsinization and ABC immunocytochemistry, keratin was found in some tumor cells of several tumors, especially in focal areas of squamous metaplasia in the adenoacanthoma (Fig. 9).

Cardiovascular System. The vasculitis involved primarily medium-size to large arteries, especially the ascending aorta. The distribution of inflammatory cells varied from multifocal to focally extensive infiltrates extending from the adventitia into the muscularis with a pattern typical of periarteritis nodosa. The perivascular inflammatory infiltrate consisted of small lympho-

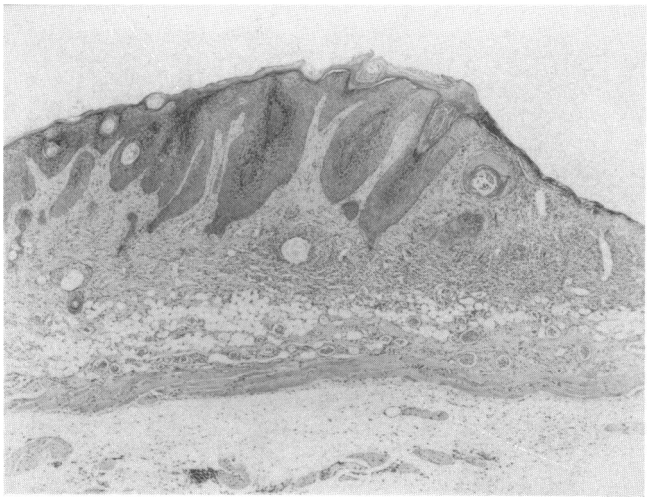

FIGURE 14. Ulcer, focal epidermal hyperplasia, and inflammation in skin of mouse after 88 weeks of TPA exposure. H & E, ×40.

cytes, lymphoblastoid cells, macrophages, a few plasma cells, and neutrophils. The adjacent media exhibited varying degrees of hypertrophy and hydropic degeneration of smooth muscle cells and fibrinoid necrosis. In several animals, this inflammatory necrotizing process resulted in fatal rupture of the vessel wall.

Endocrine System. Few mice had endocrine tumors (Table 2). The three pituitary adenomas contained abundant immunoreactive prolactin (Fig. 10). One tumor adhered to and/or invaded the brain parenchyma (Fig. 10). Pancreatic islet cell hyperplasia was seen in 35.4% of the mice. The enlarged islets contained diffuse immunoreactive insulin and focal somatostatin- and glucagon-containing cells (Fig. 11), in a pattern identical to that of normal islets.

Carcinogenesis by 12-O-Tetradecanoylphorbol-13-acetate

As part of our large skin initiation-promotion studies of formaldehyde, we had included a group of 30 female mice that received 12-O-tetradecanoylphorbol-13-acetate (TPA) for 88 weeks. At 8 weeks of age, these 30 mice received 0.2 mL acetone topically on the back. From 12 weeks of age, they received, once weekly, 1.25 μg of TPA (P. Borchert, Eden Prairie, MN) for up to 88 weeks. Mice were sacrificed at 100 weeks of age, and a complete necropsy was performed. Acetone controls were reported above as our aged acetone control mice. The clinical findings for skin papillomas and carcinomas are shown in Figure 12. Many of the papillomas apparently regressed clinically. The mean body weight of the mice in this group were similar to that of mice receiving only acetone. Two mice died or were sacrificed before week 24. Of the mice, 60% (18/30) survived past week 88 after acetone initiation (96 weeks of age). Of the 30 mice, 13 were still alive at terminal sacrifice (100 weeks of age). Histologically at the time of necropsy, seven mice had papillomas (25% of 28 mice surviving past 48 weeks) and five (17.8%) had squamous cell carcinomas (including two poorly differentiated carcinomas with areas of sarcoma) at necropsy. At least two of these carcinomas were clinically seen to arise from papillomas, and histological evidence of this was observed (Fig. 13). Several skin lesions, noted clinically, were recorded as possible papillomas or plaques that may have been regressing lesions (Fig. 14). These mice also had a variety of other tumors, including lung tumors (4 mice), pituitary tumors (2 mice), hemangiosarcoma (3 mice), Harderian gland tumors (2 mice), follicular center cell lymphoma (3 mice), histiocytic sarcoma (2 mice), mammary gland tumors (1 mouse), and tumors of miscellaneous tissues (5 mice). Two of the mice had liver, splenic, and intestinal amyloidosis.

Discussion

Female SENCAR mice used as controls in skin painting studies were quite hardy, with more than 50% surviving to 96 weeks of age, despite having serological evidence of exposure to Sendai virus and mouse hepatitis virus. Pulmonary lesions were also compatible with resolving or chronic Sendai virus lesions. The longevity of our mice appeared to be considerably longer than that of CD-1 mice, a parental strain for SENCAR mice (*5,9*). The increased survival may have been due to a low incidence of generalized amyloidosis, a major lesion in CD-1 mice (*4,9*). The tumors found in our SENCAR mice occurred with similar incidence to that in CD-1 mice with some differences (*5,9*). Histiocytic sarcomas, mammary tumors, and lung tumors were common in both stocks of mice.

The glomerulonephritis was unexpected in SENCAR mice, considering the lack of occurrence of this important disease in CD-1 mice. We did, however, find amyloid-like deposits in the nasal cavity and thyroid. Glomerular lesions were not as severe as those seen in some lupus-like syndromes but resembled lupus because of electron-dense deposits in glomerular basement membranes, vasculitis, thymic hyperplasia (*10,11*), and nephrotic syndrome in a few mice. The association of CD-1 mouse amyloidosis, abnormal immunoglobulin synthesis, and glomerulonephritis in SENCAR mice may be related to defective immune functions in these stocks of mice. The possible important role of the immune system in ultraviolet skin carcinogenesis in mice (*12,13*) suggests that the immune dysfunction in SENCAR mice may also be important for chemical carcinogenesis of the skin (*14*).

Female SENCAR mice appear to have a very high incidence of histiocytic sarcoma. This tumor, a characteristic neoplasm of mice, has been variously described as reticulum cell sarcoma Type A (*15*), histocytic lymphoma (*16,17*), and malignant schwannoma (*18*) on the basis of conventional histologic features. In female mice, these tumors often arise within the uterus. The specific cell of origin has not been identified, but tumor cells have been described as having histochemical and ultra-

structural evidence of histiocytic differentation (*16*). We could not localize common histiocytic antigens, including lysozyme and vimentin or the Schwann cell marker antigen S-100. We found α_1-antitrypsin only occasionally within tumor cells. Additional studies are needed to clarify the origin of this tumor.

Islet cell hyperplasia has been associated with obesity (*19*). Finding insulin, glucagon, and somatostatin in anatomical patterns similar to those in normal islets differentiates the enlarged, islets from adenomas, which would have single hormones or multiple hormones in an abnormal anatomical distribution (*20*).

TPA was previously reported to cause skin papillomas (*1,2,21–23*) and carcinomas (*21*) in SENCAR mice. TPA was first reported to cause skin papillomas in other strains of mice (*26–29*). Carcinomas were reported in fewer studies (*26*).

This study was supported, in part, by PHS contracts NO1-CP-41014 and CP15744 to Microbiological Associates and NO1-CO-23910 to Program Resources, Inc., from the National Cancer Institute. The aid of Cindy Harris, Kay Sheckles, Kim Forsman, Dr. Sabine Rehm, Ann Jones, Kathy Breeze, and Bob Shores is gratefully acknowledged. We thank Dr. Gurmukh Singh of the Veterans Administration Medical Center, Pittsburgh, PA, for supplying the antisera to pulmonary antigens. Dr. Beverly Cockerell of Experimental Pathology Laboratories, Inc., Herndon, VA, provided ultrastructural evaluations of some earlier renal lesions of our SENCAR mice. Dr. Sabine Rehm's expert advise is gratefully appreciated. The work described in this paper was not funded by EPA and no official endorsement should be inferred.

REFERENCES

1. DiGiovanni, J., Slaga, T. J., and Boutwell, R. K. Comparison of the tumor initiating activity of 7,12-dimethylbenz[a]anthracene and benzo[a]pyrene in female SENCAR and CD-1 mice. Carcinogenesis 1: 381–389 (1980).
2. Slaga, T. J. Overview of tumor promotion in animals. Environ. Health Perspect. 50: 3–14 (1983).
3. Boutwell, R. K. Some biological aspects of skin carcinogenesis. Progr. Exptl. Tumor Res. 4: 207–250 (1964).
4. Conner, M. W., Conner, B. H., Fox, J. G., and Rogers, A. E. Spontaneous amyloidosis in outbred CD-1 mice. Survey Syn. Pathol. Res. 1: 67–78 (1983).
5. Percy, D. H., and Jonas, A. M. Incidence of spontaneous tumors in CD^R-1 HaM/ICR mice. J. Natl. Cancer Inst. 46: 1045–1065 (1971).
6. Spangler, F., and Ward, J. M. Skin initiation/promotion study with formaldehyde in SENCAR mice. In: Formaldehyde-Toxicology, Epidemiology, Mechanisms (J. J. Clary, J. E. Gibson, and R. W. Waritz, Eds.) Marcel Dekker Inc., New York, 1983, pp. 147–158.
7. Ward, J. M., Singh, G., Katyal, S. L., Anderson, L. M., and Kovatch, R. M. Immunocytochemical localization of the surfactant apoprotein and Clara cell antigen in chemically induced and naturally occurring pulmonary neoplasms of mice. Am. J. Pathol. 118: 493–499 (1985).
8. Ward, J. M., Reynolds, C. W., and Argilan, F. Immunoperoxidase localization of large granular lymphocytes in normal tissues and lesions of athymic nude rats. J. Immunol. 131: 132–139 (1983).
9. Homburger, F., Russfield, A. B., Weisburger, J. H., Lim, S., Chak, S. P., and Weisburger, E. K. Aging changes in CD-1 HaM/ICR mice reared under standard laboratory conditions. J. Natl. Cancer Inst. 55: 37–45 (1975)
10. Andrews, B. S., Eisenberg, R. A., Theofilopoulas, A. N., Izui, S., Wilson, C. B., McConahey, P. J., Murphy, E. D., Roths, J. B., and Dixon, F. J. Spontaneous murine lupus-like syndromes. J. Exptl. Med. 148: 1198–1215 (1978).
11. Markham, R. V., Sutherland, J. C., and Mardiney, M. R. The ubiquitous occurrence of immune complex localization in renal glomeruli of normal mice. Lab. Invest. 29: 111–120 (1973).
12. Kripke, M. L. Immunologic mechanism in UV radiation carcinogenesis. Adv. Cancer Res. 34: 69–106 (1981).
13. Strickland, P. T. Tumor induction in SENCAR mice in response to ultraviolet radiation. Carcinogenesis 3: 1487–1489 (1982).
14. Outzen, H. C.. Development of carcinogen-induced skin tumors in mice with varied states of immune capacity. Int. J. Cancer 26: 87–92 (1980).
15. Furmanki, P., and Rich, M. A. Neoplasms of the Hematopoietic System. In: The Mouse in Biomedical Research. Vol. IV—Experimental Biology and Oncology (H. L. Foster, J. D. Small, and J. G. Fox, Eds.), Academic Press, New York, 1982, pp. 351–371.
16. Frith, C. H., Davis, T. M., Zolotar, L. A., and Townsend, J. W. Histiocytic lymphoma in the mouse. Leuk. Res. 4: 651–662 (1980).
17. Ward, J. M., Goodman, D. G., Squire, R. A., Chu, K. C., and Linhart, M. S. Neoplastic and nonneoplastic lesions in aging $B6C3F_1$ mice. J. Natl. Cancer Res. 63: 849–854 (1979).
18. Stewart, H. L., Deringer, M. K., Dunn, T. B., and Snell, K. C. Malignant schwannomas of nerve roots, uterus and epididymis in mice. J. Natl. Cancer Inst. 53: 1749–1758 (1974).
19. Bielschowsky, M., and Bielchowsky, F. The New Zealand strain of obese mice: Their response to stilbestrol and to insulin. Austral. J. Exp. Biol. Med. Sci. 34: 181–198 (1956).
20. Ohshima, M., Ward, J. M., and Wenk, M. L. Preventive and enhancing effects of retinoids on the development of naturally occurring tumors of skin, prostate gland and endocrine pancreas in aged male ACI/segHapBR rats. J. Natl. Cancer Inst. 74: 517–524 (1985).
21. Slaga, T. J., Klein-Szanto, A. J. P., Triplett, L. L., Yotti, L. P., and Trosko, J. E. Skin tumor-promoting activity of benzoyl peroxide, a widely used free radical-generating compound. Science 213: 1023–1025 (1981).
22. Hennings, H., Devor, D., Wenk, M. L., Slaga, T. J., Former, B., Colburn, N. H., Bowden, G. T., Elgjo, K., and Yuspa, S. H. Comparison of two-stage epidermal carcinogenesis initiated by 7,12-dimethylbenz[a]anthracene or *N*-methyl-*N'*nitro-*N*-nitrosoguanidine in newborn and adult SENCAR and BALB/c mice. Cancer Res. 41: 773–779 (1981).
23. Diwan, B. A., Ward, J. M., Rice, J. M., Colburn, N. H., and Spangler, E. F. Tumor-promoting effects of di(2-ethylhexyl)phthalate in JB6 mouse epidermal cells and mouse skin. Carcinogenesis 6: 343–347 (1985).
24. Diwan, B. A., Ward, J. M., Henneman, J., and Wenk, M. L. Effects of short-term exposure to the tumor promoter, 12-O-tetradecanoylphorbol-13-acetate on skin carcinogenesis in SENCAR mice. Cancer Letters 26: 177–184 (1985).
25. Ward, J. M., Rehm, S., Devor, D., Hennings, H., and Wenk, M. L. Differential carcinogenic effects to skin and internal tissues by intraperitoneal initiation with 7,12-dimethylbenz[a]anthracene or urethane and topical 12-O-tetradecanoylphorbol-13-acetate promotion in female SENCAR and BALB/c mice. Environ. Health Perspect. 68: 61–68 (1986).
26. Van Duuren, B. L., Sivak, C., Seidman, I., and Melchionne, S. The effect of aging and interval between primary and secondary treatment in two-stage carcinogenesis on mouse skin. Cancer Res. 35: 502–505 (1975).
27. Astrup, E. G., and Iversen, O. H. The tumorigenic and carcinogenic effect of 12-O-tetradecanoylphorbol-13-acetate when applied to the skin of BALB/cA and hairless (HR/HR) mice. Acta Path. Microbiol. Immunol. Scand. Sect. A 91: 103–113 (1983).
28. Astrup, E. I., Iversen, O. H., and Elgjo, K. The tumorigenic and carcinogenic effect of TPA (12-O-tetradecanoylphorbol-13-acetate) when applied to the skin of BALB/cA mice. Virchows Arch. B Cell Pathol. 33: 303–304 (1980).
29. Burns, F. J., Albert, R. E., and Altshuler, B. Cancer progression in mouse skin. In: Mechanisms of Tumor Promotion. Volume II. Tumor Progression and Skin Carcinogenesis (T. J. Slaga, Ed.), CRC Press, Boca Raton, FL, 1984, pp. 17–39.